On Charge Separation at the Phase Boundary Molecular Crystal/Aqueous Electrolyte

M. E. MICHEL-BEYERLE

Institut für Physikalische Chemie der Technischen Universität München

and R. HABERKORN

Physik-Department der Technischen Universität München

(Z. Naturforsch. **27 a**, 1496—1504 [1972]; received 8 August 1972)

Analysis of the electrostatics of charge carrier injection into molecular crystals during non-equilibrium electron transfer reactions demonstrates the unique advantage of aqueous or similar electrodes in measuring limiting currents which yield the rate constant of the injection process. At the phase boundary molecular crystal/aqueous electrolyte image forces are negligible due to the slow orientation polarization of water molecules with respect to the hopping frequency of injected charge carriers. Coulomb forces arising from slowly mobile or localized counter charges are shown to be effectively screened by water as a consequence of its relatively higher static dielectric constant as compared to that of the crystal.

Introduction

Hole and electron conductivity in organic homomolecular crystals of the anthracene type may originate from unipolar carrier generation (injection) at the crystal surface. Since the electronic exchange interactions between molecules in such crystals are weak (200 cm^{-1} or less) as is indicated by the low drift mobility of 1 cm^2/V sec, the injection of electrons into the lowest conduction band or, alternatively, of holes into the highest valence band can be understood as a localized electron transfer reaction in the crystal surface. At low field strength the current-voltage (j-V) dependence is limited by space charges [1], whereas it reflects the kinetics of the injection reaction at higher fields as long as these are insufficient for field emission. Electron transfer reactions, occurring at the phase boundary crystal/aqueous electrolyte yield at field strengths between 10^3 and 10^5 V/cm voltage independent limiting currents, which have been correlated to the absolute rate constant of the injection reaction [2]. In the limiting current range the applied voltage is high enough to reduce to zero the surface concentration of charge carriers, so that the current becomes saturated as long as the applied field does not affect the electron transfer reaction. The electrostatics of charge separation at the interface organic molecular crystal/aqueous electrolyte has not yet been discussed in detail except in an earlier publication [3] which attempted to account for an image potential barrier, impeding the escape of charge carriers into the bulk of the crystal.

Reprint requests to Dr. M. E. MICHEL-BEYERLE, Institut für Physikalische Chemie der Techn. Universität München, *D-8000 München 2*, Arcisstraße 21.

In the present paper the electrostatics of charge carrier injection during *non-equilibrium* photochemical electron transfer reactions will be considered with special emphasis on aqueous electrolytes as electrodes to the organic crystal. Injection processes will be formulated as photochemical electron transfer reactions, the energy of the conducting crystal states being roughly approximated by the energy of the radical ions. Charge carrier injection through the deactivation of electronically excited states can thus be understood as electron transfer between excitons [4, 5] (singlet or triplet excitons at the surface, $^1M_0^*$ or $^3M_0^*$) and electron donor (D) or acceptor (A) molecules in the aqueous phase:

$$^1M_0^*, {}^3M_0^* + D, A \xrightarrow{k_1} \underset{\downarrow E\ j}{M^{\mp} + D^+, A^-} \qquad (1)$$

or electron transfer between excited donors or acceptors (e. g. organic dyes) in the electrolyte or in adsorbed state and the crystal:

$$^{1,3}D^*, {}^{1,3}A^* + M \xrightarrow{k_2} \underset{\downarrow E\ j}{M^{\mp} + D^+, A^-}\,. \qquad (2)$$

This denotation indicates the primarily excited states and reactions products and gives no information as to the molecular interaction. The rate constants k_1 and k_2 depend on electronic energy levels (work function, ionisation energy and electron affinity) of

the crystal and reactants and are not affected by the electric field of 10^5 V/cm. With this maximum field strength the voltage drop across a lattice parameter in c' (~ 10 Å) is negligible as compared to kT in these non-equilibrium injection reactions. With increasing field strength the charge carriers are dragged away from the surface region until their concentration approaches zero on reaching the limiting current. The field strength at which the $j-V$-plot enters the limiting current is governed by the electrostatic interaction of injected charges and the electrode.

The motivation for this work arises from the possibility to discriminate through an electrochemical technique at the phase boundary molecular crystal/aqueous electrolyte quenching processes due to electron transfer from other interactions (excitation energy transfer, enhancement of internal conversion or intersystem crossing). Simultaneous to the measurement of the limiting currents, conventional spectroscopic methods are applicable for quantitative description of the different deactivation channels in heteromolecular excited systems. The phase boundary molecular crystal/aqueous electrolyte might be even relevant for biological membranes, the interface of which is as well characterized by a discontinuity of the static dielectric constant.

Experimental Results

In Figs. 1 and 2 typical $j-V$-plots for carrier injection according to reactions (1) and (2) are depicted. All measurements refer to electron injection at the ab-plane of p-chloranil (tetrachloro-p-benzoquinone) crystals, which provide clear experiments, prototypic for other molecular crystals (e. g. aromatic hydrocarbons).

Due to the high intersystem crossing rate in p-chloranil the diffusing and reacting exciton in Fig. 1 is essentially the triplet exciton, even when singlet excitons are the primarily excited species [6]. No fluorescence or appreciable long range energy transfer to the electrode have to be considered. The high energy of the triplet exciton in chloranil allows application of dye molecules as electron donors in Eq. (2) which on energetic grounds

$$\Delta E(S_0 \rightarrow S_1)_D < \Delta E(S_0 \rightarrow T_1)_M$$

are not able to populate the crystal's triplet state. Sensitized generation of triplet excitons competing

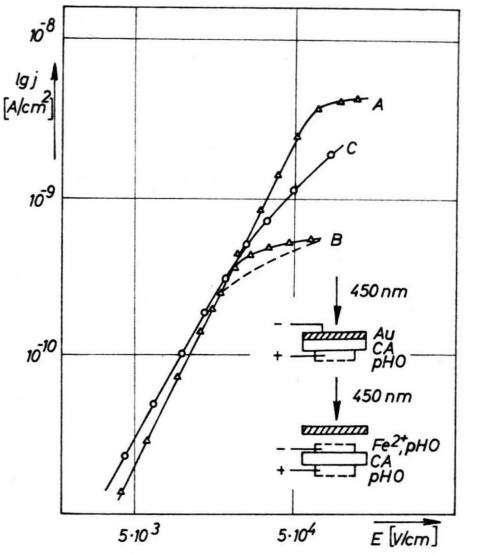

Fig. 1. Injection of electrons into p-chloranil crystals. A and B: reaction (3) at different Fe^{2+}-concentrations (10 : 1). $j_{lim,A} = j_{max} = e \varkappa I_0 L$. C: triplet exciton decay at an evaporated gold electrode. I_0 in A, B and C: $2 \cdot 10^{13}$ photons/sec cm².

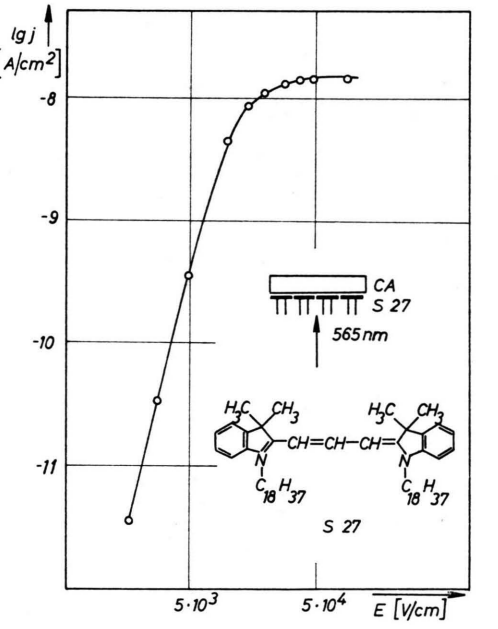

Fig. 2. Injection of electrons into p-chloranil crystals via excitation of the cyanine dye S 27 in monomolecular layer. $I_0 = 2 \cdot 10^{12}$ photons/sec cm².

with the electron transfer reaction (2) and charge carrier generation in a subsequent reaction (1) between excitons and a redox system can be excluded without further discussion. Finally oxygen does not quench triplet excitons in chloranil in a charge trans-

fer reactions leading to surface products, which could sensitively determine the phenomenology of the limiting current region of the $j-V$-plot.

The principal features of the Figs. 1 and 2 will be discussed exclusively with respect to the slope of the injection determined part of the $j-V$-plot. Experimental details and more complete treatment of the kinetics are published separately [6, 7].

Charge injection in Fig. 1 occurs according to

$$^3CA_0 + Fe^{2+} \xrightarrow{k_3} \begin{matrix} CA^- + Fe^{3+} \\ \downarrow E \\ j^- \end{matrix} \qquad (3)$$

with $^3CA_0$ representing the surface concentration of triplet excitons. For homogeneously excited n-π^*-singlet excitons which populate triplet excitons by intersystem crossing $d\varkappa < 1$ (for an extinction coefficient [6] $\varkappa = 10^2\ cm^{-1}$ at 450 nm and a diffusion length of triplet excitons [6] $L = \sqrt{D\tau} \cong 10^{-5}$ cm) and since furthermore $d/L \gg 1$ (d = crystal thickness), the limiting current can be described by the relationship [8]:

$$j_{lim} = e\,k_3[^3CA_0]\,[Fe^{2+}] = e\,\varkappa\,I_0\,L\left(1 + \frac{D}{L\,k_3[Fe^{2+}]}\right)^{-1}$$

with e = elementary charge, I_0 = light intensity, D = diffusion coefficient in the direction of the applied field ($\perp$ ab-plane) $\cong 10^{-4}\ cm^2/sec$ [6]. The expression for the limiting current is simplified, since a quenching reaction not leading to charge carriers does not occur in this case. At high concentrations of Fe^{2+}-ions (which do not inject electrons in the dark to a measurable extent), the current becomes diffusion controlled with regard to the triplet excitons and the quantum yield of reaction (3) for triplet excitons generated within their diffusion length approaches the order of unity [8a]. To illustrate the highly effective quenching process (3), the corresponding energy levels of the crystal and the redox reactant are sketched schematically in Figure 3. Exciton decay reactions yielding, under suitable conditions with equally high quantum efficiency, electron injection into chloranil as well as hole injection into anthracene crystals [8], do not support the suggestion [9], that hole ejection is less effective than electron ejection.

Because of the chemical instability of chloranil in presence of hydroxylic ions, injection experiments are preferably carried out under high proton concentration ($[H^+] = 1$ M).

It should be stated, however, that the rate constant k_3 of electron injection is not affected by the proton concentration in a wide range ($p_H\,0 - p_H\,3$). Obviously a recombination reaction according to

$$CA^- + H^+ \xrightarrow{k_4} CAH \cdot \qquad (4)$$

cannot compete with the removal of electrons from the surface in presence of a high electric field. It has been shown [2, 10] that without a sufficiently high electric field, surface products according to (4) arise. As a consequence, a slight slope gradually develops (in Fig. 1, – – – –) if one does not apply the limiting field strength prior to excitation of the crystal. The slope disappears upon rinsing the crystal with suitable solvents.

The gold filter in curves A and B has been used to allow comparison of the quantum yield of the reaction (3) with that of the analogous decay of triplet excitons at an evaporated gold contact. In the context of this paper gold seems to be especially suitable because of its high work function (Fig. 3). Gold does not inject electrons in the dark and is not involved in any kind of chemical reaction with chloranil in its electronic ground state which might deteriorate the crystal surface.

Figure 2 represents sensitized charge carrier injection

$$^1D_*^{ad} + CA \xrightarrow{k_5} D^+ + \begin{matrix} CA^- \\ \downarrow E \\ j \end{matrix} . \qquad (5)$$

At low conversion rates (N_D = const) the limiting current is given by [7]

$$j_{lim} = e\,I_0\,\sigma\,N_D \cdot k_5/(k_5 + k')$$

where σ denotes the absorption cross section and N_D the number of adsorbed dye molecules, while k' unifies the sum of deactivation steps not leading to charge carriers. At insufficient electric fields recombination according to (4) or

$$D^+ + CA^- \xrightarrow{k_6} D + CA \qquad (6)$$

will compete. In the case of Fig. 2, a cyanine dye has been applied to the crystal surface in a monomolecular layer after the technique of KUHN [11]. From the product σN_D (corresponding to 2% light absorption at 565 nm, which has been measured spectroscopically by an effect modulation technique [12]), the intensity I_0 and the limiting current j_{lim} a quantum yield in der order of unity follows for the

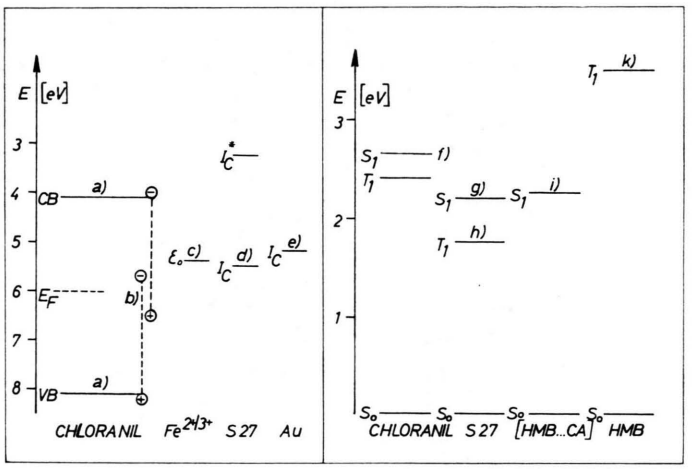

Fig. 3. Energy level diagram. a) Crystal data of chloranil are taken from Ref. [6]. Electron affinity, $EA_c = 4.1 \pm 0.2$ eV, the work function estimate as well stems from injection experiments. b) For simplicity triplet exciton energy is indicated in the one particle energy spectrum. c) Conversion of standardredox potentials vs. (NHE) into the absolute energy scale after F. LOHMANN, Z. Naturforsch. **22 a**, 843 [1967]. d) Photoemission threshold of crystalline S 27. J. KINDER, personal communication. e) Work function of spectroscopic pure gold, $I_c = 5.2$ eV after J. C. RIVIERE, Work Function Measurements and Results, Metallurgy Div. Atom. Energy Res. Etabl., Harwell 1957. f) H. P. TROMMSDORFF, P. SAHY, and J. KAHANE-PAILLOUS, Spectrochim. Acta **26** A, 1135 [1970]. Lowest excited singlet state in chloranil crystals: $n-\pi^* A_u$. g) Ref. [12]. h) Extrapolation of S_1-T_1-splitting in dyes after R. W. CHAMBERS and D. R. KEARNS, Photochem. Photobiol. **10**, 1215 [1969]. i) Ref. [13]. k) J. B. BIRKS, Photophysics of Aromatic Molecules, Wiley-Intersci., New York 1970.

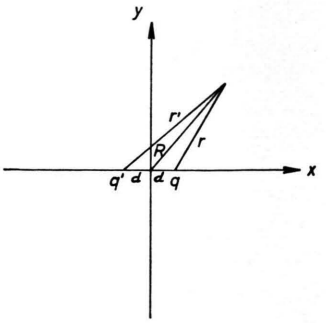

Fig. 5.

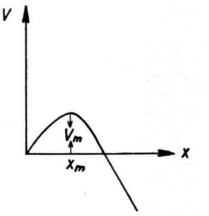

Fig. 6.

Fig. 5. Potential energy of electrons vs. distance inside crystal from electrode.

Fig. 6. Location of charge q and image charge q'.

sensitized electron injection. This high quantum yield seems possible on the basis of the energy diagram (Fig. 3), which indicates that the minimum energy condition $I_c(D) - EA_c(CA) < 0$ is even fulfilled, when an uncertainty as to the ionisation energy of the adsorbed dye in its excited singlet state $I_c(D^*)$ of ~ 0.5 eV is included.

The action spectrum of the sensitized electron current in Fig. 2 follows the absorption spectrum of the monomolecular dye layer. The spectral features are unaffected by the energy levels of the crystal, as identical sensitized hole injection and absorption spectra of the dye S 27 at the ab-plane of anthracene or perylene crystals (with $\Delta EA_c \gtrsim 2$ eV as compared to chloranil) reveal. The geometry of the ab-plane of monoclinic crystals as well as the epitaxial adsorption of dye molecules hereon [8] (as analyzed with polarized light) certainly does not favour the principle of maximum overlap of interacting orbitals in $\pi - \pi^*$-charge transfer complexes [13].

In Fig. 4 a $j-V$-dependence different from that in Fig. 2 is depicted for another kind of sensitized electron injection. In this figure, however, the donor species is an excited $\pi - \pi^*$ charge transfer complex. We will show that from the characteristic deviation of the limiting current behaviour mechanistic information as to the injection reaction might be derived. Curve A corresponds to the laser excitation of a microcrystalline layer [14] of the hexamethylbenzene-chloranil (HMB . . . CA) complex, present at the chloranil ab-plane. Since at the exciting wavelength chloranil triplet excitons are produced as well, addition of quenching ions (Fe^{2+}) to the electrolytic contacts will guarantee quantitative reaction of excitons at both interfaces according to (3). The pronounced dependence of the current in the high field region on the direction of the electric field (Fig. 4) as well as the spectral features of A, which follow the isotropic absorption spectrum of the crystalline complex, indicate that the dominant injection mechanisms in A is indeed connected to the excited charge transfer species. It should be stated that the complex does not inject electrons in the dark, although the proximity of more than one molecules of the complementary species can cause the ground state of the complex in the solid phase to have considerably more ionic character than the ground state of an isolated donor-acceptor-pair in inert environ-

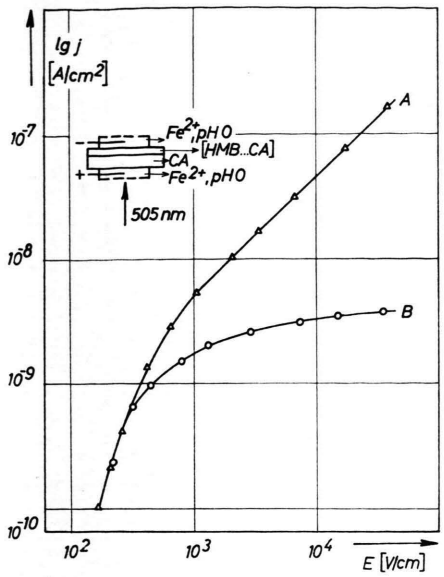

Fig. 4. Injection of electrons into p-chloranil crystals via excitation of the (HMB ... CA)-complex (A) and the reaction of homogeneously excited triplet excitons with Fe^{2+}-ions (B) at the illuminated crystal face with the direction of the electric field reversed.

ment. For weak charge transfer interactions of the Mulliken type the contribution of the charge-transfer structure in the ground state is small and charge-transfer absorption is mainly due to transition from the non-bonding ψ_0 (HMB ... CA) structure to the ionic structure ψ_1 ($HMB^{\delta+} \ldots CA^{\delta-}$). Whether injection upon excitation of the complex occurs via the overall mechanism

$$CA + {}^1(HMB \ldots CA)^* \xrightarrow{k_r} \underset{\downarrow E}{CA^-} + (HMB^+, CA) \qquad (7)$$
$$e^-$$

or via a competitive population of the system's lowest triplet state (Fig. 3)

$$CA + {}^1(HMB \ldots CA)^* \xrightarrow{k_s} {}^3CA_0 + (HMB \ldots CA) \qquad (8)$$

and subsequent reaction of triplet excitons at the crystal surface according to (3) cannot be answered without further discussion. The contribution of (7) to the injection current is, among other parameters, certainly determined by the relative polarization energies of the two ions, the resonance energy and Coulomb attraction of the ion pair in the solid phase [13].

Discussion

By the non-equilibrium reactions (3) and (6) charge carriers are generated at the distance $x = 0$ from the surface. These may migrate into the bulk of the crystal by diffusion and drift in an electric field or recombine according to (4) or (6) at the surface, thus being removed from current carrying. We assume a potential barrier (Fig. 5) at the crystal surface, which inhibits the transport of charge carriers into the interior of the crystal. The potential barrier is thought to exhibit its maximum value V_m in a distance x_m from the surface and may arise from residual space charges or from forces between the charge carriers and their image charges or real counter charges on the other side of the phase boundary.

This model has been considered in a more general way by KALLMANN and POPE [3], using the boundary condition

$$j = I - v\, n_0 \qquad (9)$$

where I represents the primary injection rate of carriers, v, a finite surface recombination velocity, n_0, the concentration of charge carriers at the surface. By simple arguments it is possible to deduce an equation for the $j-V$-plot which is identical with the general equation in Ref. [3], if suitable parameters are chosen. At a distance $x > x_m$ from the surface the current may be given solely in terms of charge carrier drift (density n_m, drift mobility μ) by

$$j = \mu\, n_m\, E\,. \qquad (10)$$

We approximate E by the externally applied field and restrict our consideration to currents beyond the space charge limited region. If one assumes that overcoming the potential barrier is a thermally activated process (diffusion against the electric field), then n_m is given by

$$n_m = n_0 \exp\{-V_m/kT\}\,. \qquad (11)$$

From Eqs. (9) – (11) we obtain for the current-voltage dependence

$$j = I E \left(E + \frac{v}{\mu} \exp\{V_m/kT\}\right)^{-1}. \qquad (12)$$

At very high field strength there is a limiting current, $j_{lim} = I$, which implies that all carriers injected contribute to the current. At field strength

$$E < E_{lim} = \frac{v}{\mu} \exp\{V_m/kT\}$$

but outside space charge limitation, one obtains a linear dependence of the $j-V$-plot

$$j = I\,E\,\frac{\mu}{v}\exp\{-V_m/kT\} = I(E/E_{lim}) \qquad (13)$$

which enters the limiting current at $E \cong E_{lim}$. Thus, the slope of the injection determined part of the $j-V$-plot and the limiting field strength E_{lim} depend strongly on the surface recombination velocity v and on the height of the potential barrier V_m. In case the limiting current cannot be reached, the highest field strength gives a lower bound for E_{lim}, whereas the slope in a linear $j-V$-plot and the number of excitons generated within their diffusion length or of excited dye molecules in adsorbed state provide an upper bond for E_{lim}.

For metals as electron donors or acceptors no limiting currents are found up to a field strength of 10^5 V/cm. In this case the exponential term in (12) should be determined essentially by image forces [14a], $\exp\{V_m/kT\} = 10^3$. An example of an $j-V$-plot obeying Eq. (13) with a proportional $j-V$ region up to high field strengths is given in Figure 1. Since the quantum yield in A approaches the order of unity and the light intensities in A and C being equal, the intersection of the proportional branch with the limiting current A gives 10^5 V/cm $< E_{lim} < 3\cdot 10^5$ V/cm and allows the tentative conclusion $v = 10^2$ to 10^3 cm/sec. A value of $v = 10^2$ cm/sec has been reported [15] for the recombination of holes at an anthracene/silver boundary, deduced from independent measurements. This value seems to be surprisingly low when compared with the thermal velocity of the charge carriers in such crystals ($v_{th} = 10^6$ cm/sec for electrons and holes in anthracene [16]).

The essential assumption of an alternative mechanism [17] for the overcoming of the image potential during injection of charge carriers is based on the initial separation of the charge carriers from the electrode. The charge carrier generation process in the bulk of an organic crystal has been earlier described [18] in terms of the ONSAGER model [19], in which electron-hole pairs are produced promptly upon photon absorption, and come to thermal equilibrium with the lattice, while still being weakly bound to the mutual Coulomb fields. Final separation into free carrires is then accomplished by thermal activation and by the external electric field.

Applying this model to surface injection of charge carriers [17], the experimentally observed photocurrent at low field strength may be given by

$$j = A(T)\,[1 + (e^3/2\,\varepsilon\,k^2\,T^2)\,E]$$
$$\text{with } A(T) = 4\,\pi \int I \exp\{-e^2/\varepsilon\,x\,kT\}\,g(x)\,dx \qquad (14)$$

where $g(x)$ gives the initial spatial distribution of thermalized carriers and ε the dielectric constant of the crystal. The equation predicts a linear field dependence for low fields and implies an initial separation of injected carriers and counter charges.

Since both models [Eqs. (13) and (14)] for electric fields $> 10^4$ V/cm predict a proportional behaviour in the $\log j - \log V$-plot, it is difficult to choose between them on the basis of the field dependence alone [18].

Recently, injection of charge carriers in the dark (equilibrium case) has also been interpreted [17] in terms of the Onsager model. We believe, that in equilibrium the Onsager mechanism should not be applicable, since this mechanism accounts only for the transition of thermalized charge carriers in distance $x < x_m$ from the surface to a state at the Fermi level of the electrode, but not for the reverse process. In equilibrium, this latter process (injection of carriers from the Fermi level of the electrode and diffusion against the potential barrier) cannot be neglected, however, by reasons of detailed balancing.

For aqueous electrolytes as contacts to the crystal in reactions (1) and (2) KALLMANN and POPE [3] postulated a similar high image force as for metals, since an image force also appears at the boundary between two dielectrics, proportional to the difference in the dielectric constants of the crystal (ε_1) and of water (ε_2):

$$\varphi = q\,\frac{\varepsilon_1-\varepsilon_2}{\varepsilon_1(\varepsilon_1+\varepsilon_2)}\,\frac{1}{r}\,.$$

A well understood example of such an image potential effect is the inhibited emission of electrons from ^{4}He into vacuum [20]. Since in the experiments with electrolytic electrodes, however, limiting currents occur already at field strengths as low as 10^3 V/cm, the limiting field strength E_{lim} is still buried in the space charge limited region and consequently a linear region does not appear. It seems therefore to be necessary to discuss again the question of an image potential in this system.

The high static dielectric constant of water of 81, which derives from the orientation polarization of the water molecules, only holds up to frequencies of 10^{11} sec^{-1} (l. c. [21]). The corresponding time con-

stant for the motion of charge carriers in an anthracene crystal is, however, the hopping frequency in the order of 10^{13} sec^{-1} (l. c. [22]). This implies that for very narrow bands, transport of carriers at room temperature takes place via hopping and electron exchange is the rate determining step.

Since lattice parameters in p-chloranil crystals [23] are still smaller as compared to anthracene, we assume the hopping frequency to be at least thta of anthracene. Thus, charge carriers do not remain long enough localized at a molecule in the surface [24], such that their potential energy can be reduced by rotation of neighbouring water molecules.

As a result, with electrolytic contacts image forces just due to the difference of the optical dielectric constants between the crystal ($n^2_{CA} \sim 4$ [6]) and the aqueous medium ($n^2_{H_2O} \sim 5$ [21]) have to be considered, i. e. image forces can be neglected in this case. Another mechanism for the appearance of an image force could consist in the displacement of ions in the aqueous phase. This seems to be unlikely since the hopping frequency of protons (with maximum mobility as compared to other ions) in water [21] is slow as compared to the motion of charge carriers in these crystals.

However, there still remains the question of the influence of the real counter charge localized at the reactants after the electron transfer step is completed. This question is of relevance in case of sensitized injection via adsorbed dye molecules, but also important for diffusing redox ions, since their velocity is small ($D \sim 10^{-5}$ cm^2/sec) in comparison with the relaxation time of water molecules. In both cases limiting currents do occur, which moreover may indicate a quantum yield of the order of unity in the examples of this paper, and which are not influenced by electrolytic conditions, favouring long lifetimes of radical counter ions on the right hand side of Equation (2).

In the following we try to show to what extent screening of counter charges by the aqueous electrolyte may be responsible for reduced Coulomb forces, exerted on the injected carriers. Since a microscopic theory requires considerably more microscopic information than is available, we resort to a continuum estimate of the screening effects due to solvent. Since we do not know whether the counter charge should be placed in the crystal (medium 1) or more inside the adjacent electrolyte (medium 2), both cases will be briefly discussed [25].

1. Charge q, located in Medium 2

The electrostatic potential in medium 1 is given by

$$\varphi_1 = \frac{q}{\frac{1}{2}(\varepsilon_1+\varepsilon_2)} \frac{1}{r} .$$

2. Charge q, located in Medium 1

In this case φ_1 originates from the counter charge q and its image charge q' (Fig. 6) according to

$$\varphi_1 = \frac{q}{\varepsilon_1 r} + \frac{q'}{\varepsilon_1 r'} \text{ with } \quad q' = q\frac{\varepsilon_1-\varepsilon_2}{\varepsilon_1+\varepsilon_2}$$

Expansion for small d:

$$\varphi_1 = \frac{q}{\frac{1}{2}(\varepsilon_1+\varepsilon_2)} \frac{1}{R} - \frac{2\,\varepsilon_2}{\varepsilon_1(\varepsilon_1+\varepsilon_2)}\; q\, d \frac{X}{R^3} .$$

Here as well as in case 1 the counter charge is screened by a factor $1/\frac{1}{2}(\varepsilon_1+\varepsilon_2)$. Furthermore, there appears a dipole term, which decreases rapidly with distance, however.

Certainly the static dielectric constant of water of 81 is not realistic in the region of the phase boundary, but there is some evidence that ε_2 might still be considerably larger than the optical dielectric constant. This assumption is supported by the bathochromic solvatochromism of adsorbed dye molecules with permanent dipole moment in the ground state [7]. Even with a reduced static dielectric constant of water at the crystal surface of $\varepsilon_2 = 15$, the exponential term in Eq. (13) decreases by more than two orders of magnitude.

From these considerations it follows that for the phase boundary crystal/electrolyte image forces are negligible due to the slow orientation polarization of water as compared to the hopping frequency of injected charge carriers. Coulomb forces arising from slowly mobile and localized charges are screened effectively by water due to its higher static dielectric constant. Both influences account for the appearance of limiting currents in Figures 1 and 2. If one assumes the potential barrier to be small in the limiting current region and a homogeneous drop of the applied field across the crystal, 10^5 V/cm yield a lifetime of radical ions in the surface between 10^{-11} and 10^{-12} sec with $x_m = 50$ Å, $d_{c'} =$ 10 Å and the microscopic drift mobility $\mu = 1$ cm^2 /V sec, assumed for the first several layers. These short lifetimes would explain, why recombination reactions according to (4) are not found to play

any role as long as high enough electric fields are applied. The possibility of elimination of ions formed in reactions (1) or (2) on the time scale of less than 10^{-11} sec implies interesting aspects for mechanistic questions in spectroscopy.

From the limiting currents as shown in Figs. 1 and 2 no information arises as to the dissipation of excess energy, e. g. as to the injection of carriers into higher or lower conducting states of the crystal. The experimental fact that the limiting current behaviour in analogous experiments is independent of the amount of excess energy rather invites the conclusion that temperature independent hot carrier injection [17] might not provide an essential fraction of the current in reactions (1) and (2). A tunnel mechanism which has been proposed recently [9] for sensitized charge carrier injection seems not to be valid in general because of the high quantum yield in the example of Figure 2. Certainly the different electrostatic conditions, as reflected in the injection-determined region of the $j-V$-plot, complicate comparison [17] of quantum yield in hot carrier injection, as postulated for sensitized injection of carriers from excited crystalline contacts [17], and sensitized injection via excited dye molecules, adsorbed from aqueous electrolyte.

The proportional increase of the current in Fig. 4 could be explained by recombination according to Equation (13). Even without knowledge of the temperature dependence, the $j-V$-behaviour would not be compatible with the behaviour predicted by the Onsager model. We conclude this from the slope/intercept ratio, which is estimated to be 10^{-2} cm/V from Fig. 4, the value to be expected from Eq. (14) being $(e^3/2\,\varepsilon\,k^2\,T^2) \sim 3\cdot 10^{-5}$ cm/V. Furthermore, hot electron injection cannot be important, since the specific $j-V$-dependence [17] is not observed.

Thus, the applicability of Eq. (13) would support reaction (7) as primary source of charge carriers, indicating that the screening properties of water do not operate at the local site of injection at the interface chloranil/crystal/polycrystalline charge transfer complex. This mechanism would imply that the charge transfer complex in excited state in the solid phase is at least thermally ionizable. Unfortunately, the quantum yield of the injection reaction cannot be measured as long as limiting currents do not occur and data concerning the diffusion length and lifetime of the ion-pair or possibly excitonic states or recombination rates of fully ionized states are not available. Nevertheless, it should be possible to infer on the injection mechanism in cases, where alternative mechanisms differ with respect to the electrostatic conditions of charge separation.

Acknowledgements

We are indebted to Dr. H. BAESSLER and Dr. H. KILLESREITER for valuable discussions and preprints, we also thank Prof. KALLMANN for critical reading of the manuscript. Financial support of the Deutsche Forschungsgemeinschaft is gratefully acknowledged.

[1] P. MARK and W. HELFRICH, J. Appl. Phys. **33**, 205 [1962].
[2] W. MEHL and J. M. HALE, in: Advances of Electrochem. and Electrochem. Eng., Ed.: P. DELAHAY and C. N. TOBIAS, Interscience, New York 1966. Treatment of outer sphere redox reactions at the interface crystal/electrolyte based on the Marcus-Hush approach for adiabatic electron transfer reactions.
[3] H. KALLMANN and M. POPE, J. Chem. Phys. **36**, 2482 [1962].
[4] M. POPE and H. KALLMANN, Nature **186**, 31 [1960].
[5] J. M. HALE and W. MEHL, Electrochim. Acta **13**, 1483 [1968].
[6] R. BRICKL, W. HARENGEL, H. KILLESREITER, and M. E. MICHEL-BEYERLE, to be published in Ber. Bunsenges. Phys. Chemie.
[7] R. BRICKL, M. E. MICHEL-BEYERLE, and D. MÖBIUS, to be published.
[8] M. E. MICHEL-BEYERLE and F. WILLIG, Chem. Phys. Lett. **5**, 28 [1970].
[8a] $k_3 = 10^5$ cm^4 mole^{-1} sec^{-1}.
[9] H. KILLESREITER and H. BAESSLER, Chem. Phys. Lett. **11**, 412 [1971].
[10] M. E. MICHEL-BEYERLE and F. WILLIG, Solid State Comm. **7**, 913 [1969].
[11] H. BÜCHER, O. v. ELSNER, H. KUHN, D. MÖBIUS, P. TILLMANN, and J. WEIGAND, Z. Phys. Chem. N.F. **65**, 152 [1969].
[12] H. P. BRAUN, Thesis in preparation, Technische Universität München.
[13] R. S. MULLIKEN and W. B. PERSON, Molecular Complexes, J. Wiley-Interscience, New York 1970.
[14] The complex is deposited at the crystal surface by evaporation from ligroin solution with poor solubility for chloranil (0.0001 M/l). Since the complex layer is thin as compared to the crystal (1/1000), we neglect inhomogenities of the electric field.
[14a] According to Ref. [3] we assume for V_m a value of $\sim$ 0.2 eV.
[15] C. BOGUS, Z. Physik **207**, 281 [1968].
[16] F. GUTMANN and L. E. LYONS, Organic Semiconductors, John Wiley, New York 1967.
[17] H. KILLESREITER and H. BAESSLER, Phys. Stat. Sol., in press.
[18] R. H. BATT, C. L. BRAUN, and J. F. HORNIG, J. Chem. Phys. **49**, 1967 [1968].
[19] L. ONSAGER, Phys. Rev. **54**, 554 [1938].
[20] G. W. RAYFIELD and W. SCHOEPE, Phys. Lett. **34 A**, 133 [1971].

[21] D. EISENBERG and W. KAUZMANN, The Structure and Properties of Water, Clarendon Press, Oxford 1969.
[22] R. W. MUNN and W. SIEBRAND, J. Chem. Phys. **53**, 3343 [1970].
[23] S. S. C. CHU, G. A. JEFFREY, and T. SAKURAI, Acta Cryst. **15**, 661 [1962].
[24] In the above treatment the effect of trapping has not been considered, since charge carriers located in traps cannot easily recombine with the source.
[25] L. D. LANDAU and E. M. LIFSCHITZ, Lehrbuch der Theoretischen Physik, Elektrodynamik der Kontinua, Akademie-Verlag, Berlin 1971.

Die flammenspektralphotometrische Analyse des Spurenelementes Rubidium in Graniten und deren Biotiten

ANSELM ZÄNKERT und WILHELM ACKERMANN

II. Physikalisches Institut der Universität Gießen

(Z. Naturforsch. **27 a**, 1504–1507 [1972]; eingegangen am 13. Juli 1972)

The Flamephotometric Analysis of the Trace Element Rubidium in Granites and Biotites

Rubidium determinations of granites and biotites were performed by flamephotometric measurements and controlled by isotope dilution method. For isotope geological work the flamephotometric determination is not precise enough to replace the isotope dilution technique.

Um für die Altersbestimmung von Gesteinen eine hinreichend genaue Methode zur quantitativen Analyse des Spurenelementes Rubidium zu finden, haben die Verfasser am gleichen Material Rb-Bestimmungen sowohl mit dem Flammenspektralphotometer [1–3] als auch durch Isotopenverdünnung ausgeführt.

Das Flammenphotometer wurde für unsere Messungen in Emissionstechnik betrieben. Diese Technik wird als bekannt vorausgesetzt und hier nicht beschrieben.

Arbeitsbedingungen

Hinsichtlich der Ermittlung günstigster Arbeitsbedingungen wurden eine Reihe Vorversuche unternommen, die sich neben der anzuwendenden Technik (Emission/Absorption) auf den Fremdioneneinfluß, das Aufschlußverfahren und die Alkalikonzentration erstreckten. Es ergaben sich hierbei folgende optimale Bedingungen für die Rb-Bestimmung:

1. Messung der 780 nm-Linie in Emissionstechnik.
2. Verwendung von Acetylen-Luft-Flamme in Vorkammerzerstäubung bei einem Brenngasdruck von 0,5 atü mit Heißkammer und 3 atü Luftdruck.
3. Betrieb bei voller Verstärkung und einer Spaltbreite von 0,2 mm für Gesamtgestein und 0,13 mm für Biotit.
4. Alkalikonzentrationsbereich zwischen 0 – 10 mg/l und
5. Zugabe geeigneter Mengen von Caesiumchlorid-Aluminiumnitrat-Pufferlösung zur Unterdrückung der Anregungsbeeinflussung und Standardisierung der physikalischen Eigenschaften der Meßlösung [4].

Sonderdruckanforderungen an Dr. W. ACKERMANN, II. Physikalisches Institut der Universität Gießen, *D-6300 Gießen*, Arndt-Straße 2.

Ausführung der Messungen

1. Aufnahme der Eichkurve

Zur Eichung des Flammphotometers für die Rb-Bestimmungen wurden Eichkurven erstellt (Abb. 1 u. 2). Mit Hilfe einer Heißkammer (B e c k m a n 105250 La-

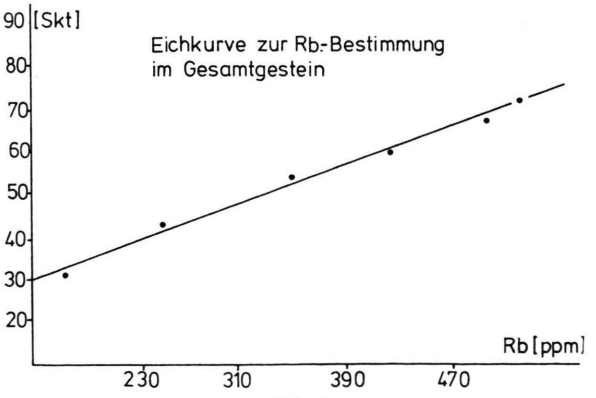

Abb. 1.